MIXED CONVECTION AND RADIATION IN A PARTITIONED ENCLOSURE WITH A MOVING WALL

Alejo, Sánchez A., and Iris, Jiménez de P.
Escuela de Ingeniería Mecánica
Universidad de Los Andes
Mérida, 5101, Mérida
Venezuela

Antonio Campo
College of Engineering
Idaho State University
Pocatello, Idaho,U.S.A

ABSTRACT

In the present paper, a numerical model is implemented in order to simulate the combined effects of conduction, radiation, and mixed convection that take place in a rectangular cavity with a moving wall in the presence of heat generating protrusions.

The problem is solved by means of a control–volume based transport model and a radiation model based on the discrete ordinates scheme. The formulation and implementation of the model, as well as the treatment of the different boundary conditions, are discussed in the paper.

Streamlines, isotherms, and radiative and/or convective local and mean Nusselt numbers are presented for some selected examples. These examples include pure convection for single protrusion with different aperture ratios ($1/3 \leq A_p \leq 2/3$) and different Rayleigh numbers ($0.0 \leq Ra \leq 3.55x10^5$) for fixed Reynolds number (Re = 100); and multiple partitions ($1 \leq N \leq 4$) for fixed aperture ratio ($A_p = 2/3$) and fixed Rayleigh and Reynolds numbers ($Ra = 3.55x10^5$ and Re = 100). Also included is an example of combined radiation, conduction and mixed convection in the presence of a heat generating protrusion.

Comparisons with earlier published results are made whenever possible.

NOMENCLATURE

A_p	Aperture Ratio
E	Energy Balance Defined by Eq. 23
I	Radiation Intensity
I^+	Boundary Intensity Defined by Eq. 14
I_b	Blackbody Intensity
k_f	Thermal Conductivity of the Fluid
ks	Thermal Conductivity of the Solid
L	Length of the Walls
L_x	Dimension of the Component in the x Direction
L_y	Dimension of the Component in the y Direction
N	Number of Partitions
Nu_{av}	Average Nusselt Number $[(Nu_c + Nu_h)/2]$
Nu_c	Convective Nusselt Number at the Cold Wall (Eq. 20)
Nu_h	Convective Nusselt Number at the Hot Wall (Eq. 20)
Nu_{rc}	Radiative Nusselt Number at the Cold Wall (Eq. 20)
Nu_{rh}	Radiative Nusselt Number at the Hot Wall (Eq. 20)
Nuu	Convective Nusselt Number at the Upper Wall
Nul	Convective Nusselt Number at the Lower Wall
Pr	Prandtl Number
q_r	Net Radiation Heat Flux
$\dot{q}$	Component's Heat Generation (w/m^3)
$\bar{Q}$	Dimensionless Heat Generation $[\dot{q} L^2/k_f(T_h - T_c)]$
Ra	Rayleigh Number
Re	Reynolds Number (UL/ν)
T	Local Temperature
T_c	Temperature of the Cold Wall
T_f	Fluid Temperature
T_h	Temperature of the Hot Wall
T_i	Temperature at the Interface Component-Fluid
T_s	Temperature in the Solid
U	Velocity of the Moving Wall
$\bar{u}$	Dimensionless Velocity in x $[uL/\alpha]$
$\bar{v}$	Dimensionless Velocity in y $[vL/\alpha]$

α Thermal Diffusivity of the Fluid
β Extinction Coefficient
$\nabla \cdot \bar{q}_r$ Divergence of the Radiative Heat Flux
ε Wall Emittance
ψ Maximum Stream Function
ρ Fluid Density
ρ_d Wall Reflectance
θ Dimensionless Temperature $[(T - T_c)/(T_h - T_c)]$
ξ Dimensionless Distance in the x Direction
η Dimensionless Distance in the y Direction
ν Kinematic Viscosity
ω Solid Angle

INTRODUCTION

The problem of combined conduction and mixed convection that takes place in a rectangular cavity with protrusions and a moving wall finds application in several branches of science (geophysical, environmental, etc.) and engineering (transportation, thermal treatments, lubrication., heating and air conditioning, electronic cooling, etc).

The interaction of radiation, convection, and conduction in lid driven cavity problems found in electronic cooling has been an important area of research during the past few years (Sánchez et al., 1993b; Sánchez et al., 1994a and 1994b). This research, however, has been limited to the case of adiabatic boundary conditions The work presented in this paper is an initial step toward a more complete investigation involving the same type of problems, but under isothermal boundary conditions.

Pure natural convection in rectangular cavities containing dividers has been widely studied (Batchelor, 1954; Duxbury, 1979; Lin and Bejan, 1983; Nansteel and Grief, 1986; Zimmerman and Acharya, 1987; and Chuang et al., 1993; among many others).

The bidimensional lid-driven cavity flow problem has also been extensively studied (Gosman et al., 1969; Torrance et al., 1972; Morzynski and Popiel, 1988; Mohamad and VisKanta, 1991; Ramesh and Lean, 1992; Iwatsu et al., 1992; among others).

The inclusion of heat generating protrusions, even in the absence of radiation, increases the numerical difficulty of the problem and only a few solutions are reported in the literature (Papanicolau and Jaluria, 1990 and 1991). Moreover, and to the best of our knowledge, there is only one publication (Sánchez et al., 1993a), where the effects of radiation in lid-driven cavity flows –without heat generating protrusions– has been studied; and only a few where the full problem has been undertaken (Sánchez et al, 1993b; and Sánchez et al., 1994a). These works, however, were limited to adiabatic boundary conditions.

In this paper, a numerical model allowing for the solution of the conjugated problem is presented. Next, the model is implemented in order to solve some particular cases related to multiple partitions and different flow conditions. Latter, an example is given in order to show the full potential of the method. Finally, conclusions about the validity of the model and the future development in this line of research are given.

DESCRIPTION OF THE MODEL

Figure 1 shows a general square cavity with black, diffuse walls of length L. For the case shown in Figure 1a, the lateral walls are adiabatic and the horizontal walls have temperatures T_h and T_c with $T_h > T_c$. For the case shown in Figure 1b, on the other hand, the vertical walls are isothermal (with $T_h > T_c$) and the horizontal walls have a lineal temperature distribution. The upper wall (could be an air current), moving with a velocity U, induces a laminar flow on the fluid contained in the cavity which is positioned in such a way that the force of gravity acts parallel to the vertical walls. Except for the density in the buoyancy term, the properties of the non-participating gas contained in the cavity are assumed to be constant, and the Boussinesq approximation applies. One or more electronic components or cards, with a certain heat generation $\dot{q}$ (w/m^3) and dimensions L_x and L_y are mounted on the lower wall.

Governing Equations, Nusselt Numbers, and Energy Balance

Transport Equations. For laminar flow and steady-state conditions with all the properties of the fluid assumed constant except for the density related to the buoyancy effect (Boussinesq approximation in the y momentum equation), the transport equations for 2-D flow are:

Continuity:

$$\frac{\partial}{\partial \xi}\left(\bar{u}\right) + \frac{\partial}{\partial \eta}\left(\bar{v}\right) = 0 \qquad (1)$$

x-momentum:

$$\frac{\partial}{\partial \xi}\left(\bar{u}\,\bar{u}\right) + \frac{\partial}{\partial \eta}\left(\bar{u}\,\bar{v}\right) = \Pr\left[\frac{\partial}{\partial \xi}\left(\frac{\partial \bar{u}}{\partial \xi}\right) + \frac{\partial}{\partial \eta}\left(\frac{\partial \bar{u}}{\partial \eta}\right)\right] - \frac{\partial \bar{P}}{\partial \xi} \qquad (2)$$

y-momentum:

$$\frac{\partial}{\partial \xi}\left(\bar{v}\,\bar{u}\right) + \frac{\partial}{\partial \eta}\left(\bar{v}\,\bar{v}\right) = \Pr\left[\frac{\partial}{\partial \xi}\left(\frac{\partial \bar{v}}{\partial \xi}\right) + \frac{\partial}{\partial \eta}\left(\frac{\partial \bar{v}}{\partial \eta}\right)\right] - \frac{\partial \bar{P}}{\partial \eta} + \mathrm{Ra}\,\Pr\,\theta \qquad (3)$$

energy:

$$\frac{\partial}{\partial \xi}\left(\bar{u}\,\theta\right) + \frac{\partial}{\partial \eta}\left(\bar{v}\,\theta\right) = \frac{\partial}{\partial \xi}\left(\frac{\partial \theta}{\partial \xi}\right) + \frac{\partial}{\partial \eta}\left(\frac{\partial \theta}{\partial \eta}\right) + \bar{Q} \qquad (4)$$

In the previous equations ξ and η are dimensionless distances in the x and y directions respectively; velocities are

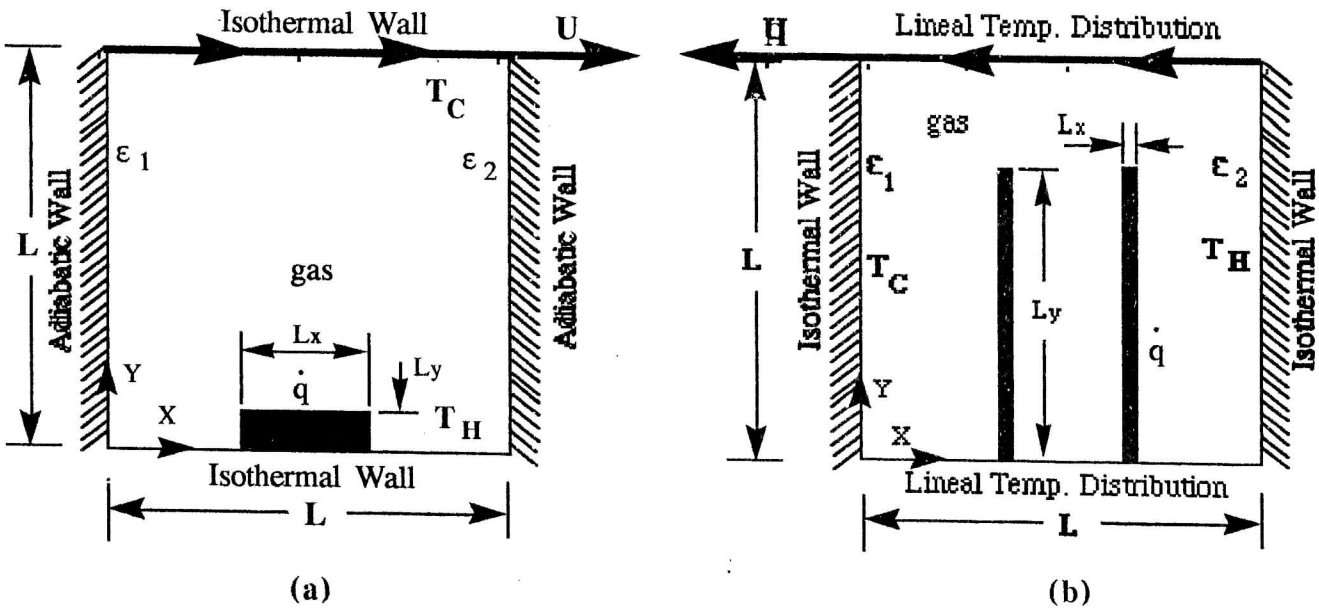

Figure 1 GENERAL GEOMETRY

normalized with α/L and the pressure is normalized with $\rho \alpha^2/L^2$; θ represents $(T - T_c)/(T_h - T_c)$; Pr y Ra are the Prandtl and Rayleigh numbers respectively. The fluid properties are taken as ρ for density, α for thermal diffusivity and k_f for thermal conductivity. T is the fluid temperature. Finally, $\bar{Q}$ represents the dimensionless heat generation defined as $\dot{q}\, L^2/k_f(T_h - T_c)$ where $\dot{q}$ is known in the electronic component, and zero everywhere else in the numerical domain.

For the case shown in Figure 1a, Equations 1-4 are subjected to the following boundary conditions

$$\xi = 0; \quad \bar{u} = 0; \quad \bar{v} = 0; \quad \frac{\partial \theta}{\partial \eta} = \frac{q_r(0)\, L}{k_f\,(Th - Tc)} \tag{5}$$

$$\xi = 1; \quad \bar{u} = 0; \quad \bar{v} = 0; \quad \frac{\partial \theta}{\partial \eta} = \frac{q_r(1)\, L}{k_f\,(Th - Tc)} \tag{6}$$

$$\eta = 0; \quad \bar{u} = 0; \quad \bar{v} = 0; \quad \theta = \theta_h \tag{7}$$

$$\eta = 1; \quad \bar{u} = Re\, Pr; \quad \bar{v} = 0; \quad \theta = \theta_c \tag{8}$$

where Re is the Reynolds number defined as $Re = U\, L/\nu$, ν being the kinematic viscosity of the medium, and q_r is the net heat due to radiation to be defined later.

On the other hand, for the case shown in Figure 1b, Equations 1-4 are subjected to the following boundary conditions

$$\xi = 0; \quad \bar{u} = 0; \quad \bar{v} = 0; \quad \theta = \theta_h \tag{9}$$

$$\xi = 1; \quad \bar{u} = 0; \quad \bar{v} = 0; \quad \theta = \theta_c \tag{10}$$

$$\eta = 0; \quad \bar{u} = 0; \quad \bar{v} = 0; \quad \theta = \text{Lineal} \tag{11}$$

$$\eta = 1; \quad \bar{u} = Re\, Pr; \quad \bar{v} = 0; \quad \theta = \text{Lineal} \tag{12}$$

Radiative Transfer. The propagation of radiation (I) along a line-of-sight direction ζ is described by the radiative transfer equation. Without scattering, the change in the radiant intensity $I(\zeta)$ in the $\bar{\omega}$-direction is expressed by

$$\frac{dI}{d\zeta} = -\beta\, I(\zeta) + a\, I_b \tag{13}$$

In Equation (13), β is the extinction coefficient given by the sum of the absorption coefficient (a) and scattering coefficient (s) which are both zero when the working fluid is air. Equation 13 is subject to the following boundary conditions

$$I^+ = \varepsilon\, I_b^+ + \frac{\rho_d}{\pi} f_d \int_0^{2\pi} (I^-(\bar{\omega}_i)\, \eta\, d\omega^-) + \rho_d\,(1 - f_d)\, I_m^- \,. \tag{14}$$

In Equation 14, superscripts + and - indicate radiation going from the boundary toward the medium inside the domain, and from the medium toward the boundary, respectively. The boundary has an emittance ε and blackbody intensity I_b which depends on the temperature of the surface. The reflectance of

the boundary is denoted by ρ_d, which, for convenience, is taken to be independent of direction. The fraction of the reflection that is diffuse is f_d. The cosine of the angle between the direction of propagation of $\bar{I}$ and the normal to the given boundary is η. The intensity in the direction mirroring the direction of $\bar{I}$, that is, the specularly reflected intensity, is $\bar{I}$,m). Physically, the terms on the right-hand-side of Equation 14 represent emission, diffuse reflection of incident intensity from within the medium, and specular reflection of incident intensity. The expression in Eq. 14 could be modified to account for bidirectional reflectance and transmittance distribution functions. The intensity I_b^+ is assumed known.

The divergence of the radiative flux (which is zero when the working fluid is air) is expressed as

$$\nabla \cdot \bar{q}_r = a\,\pi\, I_b - a \int_0^{4\pi} I_\lambda(\bar{\omega})\, d\omega \qquad (15)$$

where a is the monochromatic absorption coefficient , I_b is the monochromatic blackbody intensity evaluated using Planck's law, I is the radiant intensity for the $\bar{\omega}$-direction, and ω is the solid angle. The dependency of a, I_b, and I on the spatial variables is understood.

The net heat flux on a given surface is expressed as

$$q_r = \int_{4\pi} I\, \eta\, d\zeta \qquad (16)$$

Component-Fluid Interface (Internal boundaries). The treatment given to the component-fluid interface requires particular attention. This interface is shown in Figure 2 where two adjacent control volumes, one in the solid component and another in the contiguous fluid, are represented.

In Figure 2 T_f and T_s are the average temperature for the control volumes corresponding to the fluid and the solid side respectively, and δ_f y δ_s are the corresponding distances from center to boundary. q_r is the net radiative flux leaving the component through the specified control volume.

An energy balance at the boundary indicates that the temperature of the interface (needed by the radiative model) can be written as

$$T_i = \frac{\frac{k_s}{\delta_s} T_s + \frac{k_f}{\delta_f} T_f - q_r}{\frac{k_s}{\delta_s} + \frac{k_f}{\delta_f}} \qquad (17)$$

where k_s and k_f are the thermal conductivities for the solid and the fluid, respectively.

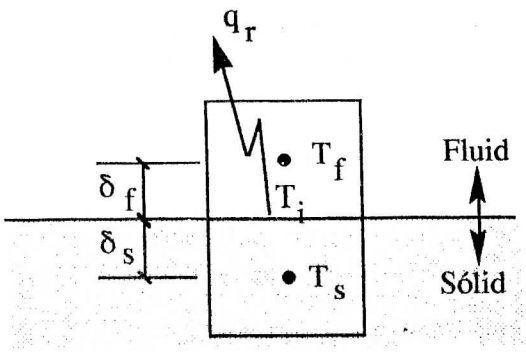

Figure 2 INTERFACE COMPONENT-FLUID

Similarly, an energy balance on the control volume situated in the solid side indicates that Equation 4 should be modified, for these interface-control-volumes, substituting $\bar{Q}$ by

$$\bar{Q} - \bar{q}_r \qquad (18)$$

where

$$\bar{q}_r = \frac{q_r L^2}{k_f (T_h - T_c)} \qquad (19)$$

Nusselt Numbers and Energy Balance. At the hot or cold wall , the convective Nusselt number was evaluated (Sánchez et al., 1992) as

$$Nu_{h \text{ or } c} = -\frac{q''(h \text{ or } c)\, L}{k_f (T_h - T_c)} = -\int_0^1 \left.\frac{\partial \theta}{\partial \eta}\right|_{\eta=0} d\xi \qquad (20)$$

where q" is the average heat flux per unit area, due to convection alone, on the wall being considered. It should be noticed that Equation 20 is equally used in regions where the component or the fluid are present. In the former case, therefore, an equivalent "conductive" Nusselt is being defined.

Similarly, the Nusselt numbers due to radiation are defined as

$$Nu_{rh \text{ or } rc} = -\frac{q_r(h \text{ or } c)\, L}{k_f (T_h - T_c)} \qquad (21)$$

In the absence of internal heat generation, the summation of Equations 20 and 21 should produce zero. When internal heat generation is considered, however, the energy balance (E) should include this term as

$$E = \sum Nu + \frac{\bar{Q} L_x L_y}{L^2} \qquad (22)$$

Or more restrictive

$$E = \frac{|q_{net}|}{q_{in}} \quad \text{(in \% of } q_{in}) \quad (23)$$

where

$$q_{net} = + q'_h + q'_c + q'_{rh} + q'_{rc} - \dot{q}\, Lx\, Ly \quad \text{(in W/m)} \quad (24)$$

and

$$q_{in} = \dot{q}\, Lx\, Ly + \Sigma\,(q_h)_{only\ positive} + \Sigma\,(q_c)_{only\ positive} \quad (25)$$

NUMERICAL PROCEDURE

The transport and energy equations were solved using a control volume approach (Patankar, 1980). On the other hand, the radiative transfer algorithm used in the last test of this study is based on the discrete ordinates model, and it has built in the possibility of solving for non-homogeneous media (ANDISORD4, Sánchez, et al., 1992). Following recommendations from other studies related to radiative transport in transparent media (Sánchez and Smith, 1992), the discrete ordinates algorithm was implemented with an equally spaced, equally weighted quadrature set and a finite-difference factor of 0.6.

When the working fluid is a nonparticipating medium, the transport equations and the radiative transfer equation are explicitly decoupled. Their solution, however, is implicitly interdependent trough the boundary conditions.

Serious convergency problems have already been reported for the type of geometry being studied here (in the absence of radiation –Papanicolau and Jaluria, 1991–), and similar limitations have been reported in partitioned cavities without moving boundary or heat generation (with radiation –Yucel and Acharya, 1990–, and without it –Chuang et al., 1993–). Steady state conditions (when they exist) are reached after a long period of instability that requires low underrelaxation factors and, consequently, hundreds and even thousands of iterations.

Based on the sensitivity analysis for the grid reported in Sánchez et al., 1993a, it was decided to use an uniform 42x42 grid mesh. However, due to the presence of heat generating protrusions (like in the last test) and the instability problem reported above, a finer, non-uniform grid seems advisable. For the preliminary results reported here, it was not considered advisable to further increase the computational effort and the 42x42 uniform grid mesh was maintained. Even with this limitation, an averaged wall clock time of two minutes per convection-radiation-iteration and 30 seconds for a pure-convection-iteration was needed on a personal computer with a typical experiment –changing only one parameter– requiring about 1500 iterations.starting from a previously converged, related, problem).

A given experiment was considered converged when none of the variables changed, between successive iterations, in more than $1x10^{-4}$ and the summation of the residual mass was less than $1x10^{-5}$. Depending on the experiment, the relaxation factor toke values between 0.1 and 0.6.

RESULTS

A series of experiments where performed in order to study the influence of several parameters on the heat transfer rate. Unless other indication is given, all experiments where conducted for $k_f = 0.03$, $k_s/k_f = 2$, $Re = 100$ and $Pr = 0.71$.

Test 1: Mixed Convection Without Radiation

For the geometry shown in Figure 1b, the aperture ratio (Ap) is defined as (L-Ly)/L. Several tests were performed for Lx = 0.05 L, with $1/3 \le A_p \le 2/3$ and for different flow conditions. In all cases the protrusions were considered without heat generation. Some representative streamlines and isotherms are shown in Figures 3 and 5. The three numbers appearing on top of each figure indicate the maximum, the spacing, and the minimum of the variable being represented.

For pure natural convection (Figure 3a) the maximum streamline value reported here ($\psi = 27.94$) compares very well with that reported by Chou et al., 1993, ($\psi = 27.87$) for the same problem. This result is particularly good considering that Chou et al., 1993, used a 56 x 44 non uniform grid.

Figure 4 shows the average Nusselt numbers at the cold (Nuc), hot (Nuh), upper (Nuu), and lower (Nul) walls for pure natural convection (Re = 0), for the upper wall moving from left to right (Re = 100) and for the upper wall moving from right to left (Re = -100). Also shown in this figure are the conductive "Nusselt number" related to the heat conducted through the bottom part of the protrusions, and the average Nusselt number (defined as (Nuc + Nuh)/2)). As can be seen in this figure, the heat transfer from the top of the enclosure increases considerably when the upper layer moves from right to left forcing the fluid to move more vigorously. On the other hand, when movement of the upper layer from left to right forces the fluid to move against the natural direction of flow resulting in a decrease of the heat transfer through the upper wall.

Figure 6 shows the effect of the Rayleight number on the heat transfer due to mixed convection that takes place in an enclosure with Ap = 2/3 and with the upper lid moving from right to left (Re = 100). It is clear that, in general, the heat transfer rate increases with increasing Ra.

Figure 7 shows the influence of Ap over the average Nusselt number for a cavity with a single partition and Re = 100 (lid moving from right to left). It can be seen that as Ap increases so does the average Nusselt number. Also shown in this figure are some values of Nuav available from other researchers for the case of pure natural convection. As can be seen, even a weak intensity of the lid forcing can result in a noticeable increase of the average Nusselt number for low to middle aperture ratios. As the Ap increases, the effect of forced convection decreases.

Finally, Figure 8 shows how the average Nusselt number for an enclosure with Ap = 2/3 and Re= 100 decreases as the number of partitions increases. Also shown in this figure are the numerical results of Chuang et al., 1993, for pure natural

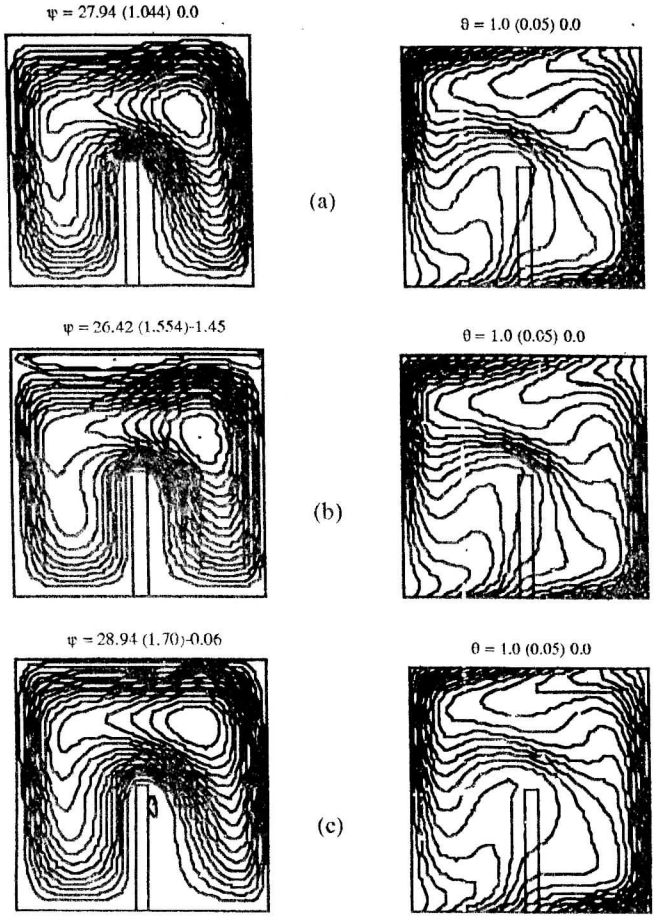

Figure 3 STREAMLINES AND ISOTHERMS FOR AN ENCLOSURE WITH A_P = 1/2 AND Ra = 3.55 x10^5 (Re = 0.0 in (a); Re = 100 –lid moving from left to right–in (b) ; and Re = 100 –lid moving from right to left–in (c))

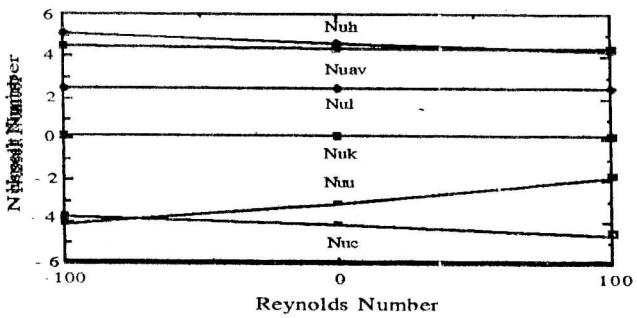

Figure 4 NUSSELT NUMBERS vs REYNOLDS FOR AN ENCLOSURE WITH A_P = 1/2 AND Ra = 3.55 x10^5 (Re = -100 –lid moving from left to right– and Re = 100 –lid moving from right to left–)

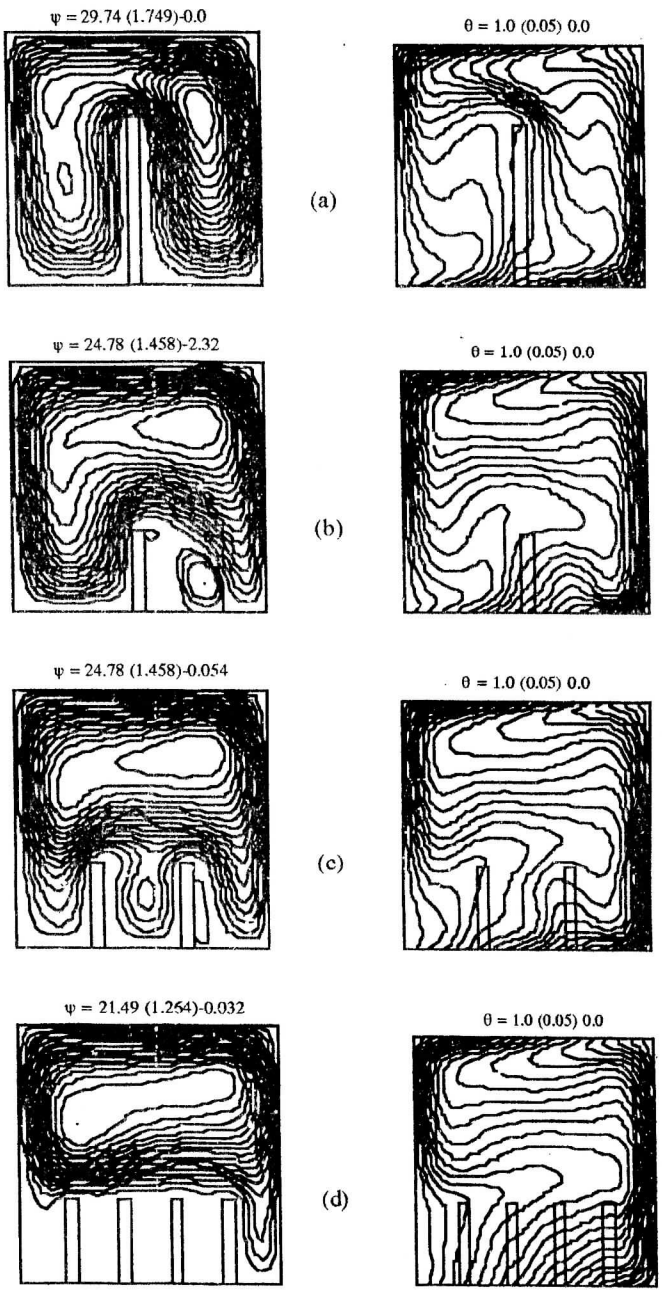

Figure 5 STREAMLINES AND ISOTHERMS FOR AN ENCLOSURE WITH Ra = 3.55 x10^5 and Re = 100 –lid moving from right to left–. A_P = 1/3 in (a) and 2/3 in (b), (c), and (d).

convection. It can be seen that as the number of protrusions increases, the effect of forced convection becomes more noticeable as an aid to heat transfer.

Test 2: Mixed Convection With Radiation

In order to show the full potential of the model, a final test was performed for Lx = 0.095 L and A_p = 0.62. In this test the card has a heat generation $\bar{Q}$ = 1000 and the Reynolds number is taken as 100. Some other parameters for this test are: k_f = 0.03, k_s/k_f = 10, Pr = 1, Ra = 0.0, T_H = 300 K,Tc = 0.9T_H K and all the walls are assumed as black and diffuse (just for simplicity since the model allows for gray or even specular walls).

Some representative streamlines (exponentially separated) and isotherms (equally spaced) are shown in Figure 9a and 9b.

The main results from this experiment were: maximum streamline - 8.776 (in point x in Figure 9a); maximum dimensionless temperature of the card 0653594 (in point x in Figure 9b); Nu_u= -3.56 Nul = 1.31, Nu_{ru} = -1.4.8, Nu_{rl} = 77.65 (where Nu_{ru} and Nu_{rl} are the Nusselt numbers due to radiation on the upper and lower surfaces respectively); the equivalent Nusselt number due to conduction through the base of the card was found to be -1.28; and energy was conserved within a 0.5% according to Equation 23.

It is important to notice the relative importance of radiative cooling with its convective counterpart –up to two orders of magnitude–. Radiative transfer is, for this particular case, the main cooling mechanism.

CONCLUSIONS

A model that allows for the numerical simulation of combined radiation, conduction and mixed convection in lid driven cavity flows has been presented.

The model has been tested in different situations ranging from pure forced to pure natural convection, and in cases including one or more partitions; protrusions with or without heat generation; and Rayleigh numbers ranging from 0 to $3.55x10^5$. In all the cases presented, the model behaved correctly and the results obtained, when compared with results from other authors, seem plausible.

The relative importance of the different modes of heat transfer have been discussed for the tests presented in this work. Of particular importance is the fact, demonstrated in the final test, that radiation can be the dominant mechanism of heat transfer for this type of applications, even at low temperatures.

Finally, it is important to point out –given the nature of this congress– that the model presented here can be applied – and in fact it has been done– to problems related to atmospheric circulation, stratification, air conditioning, channel flows, etc. Also, the model can be easily extended to include turbulent fluid flows

REFERENCES

Batchelor, S. M.,1954, "Heat Transfer by Free Convection across a Closed Cavity between Vertical Boundaries at Different Temperature," Q. Appl. Math., Vol. 12., pp. 209-233

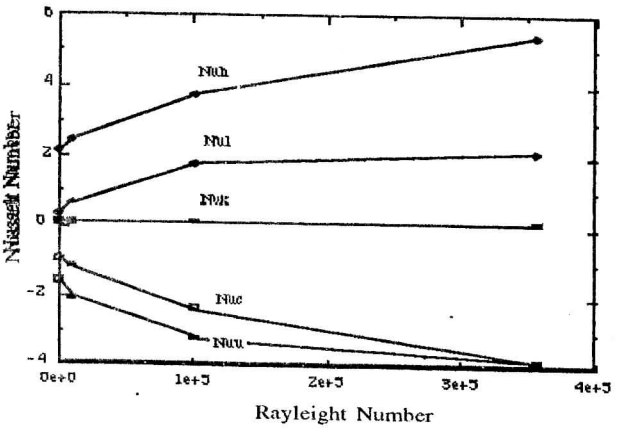

Figure 6 NUSSELT NUMBER vs RAYLEIGHT NUMBER FOR AN ENCLOSURE WITH A_p = 2/3

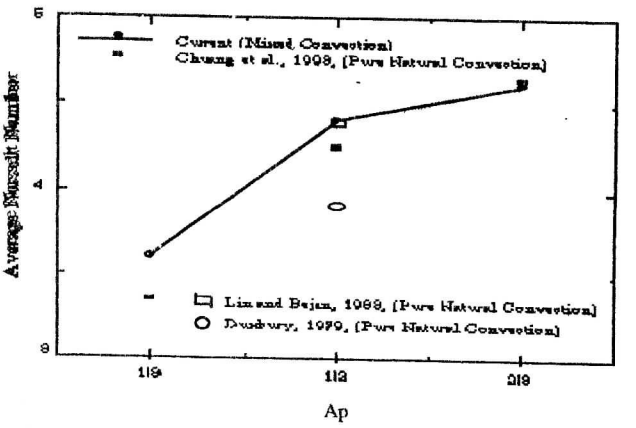

Figure 7 AVERAGE NUSSELT NUMBER vs A_p FOR AN ENCLOSURE WITH Ra = $3.55x10^5$.

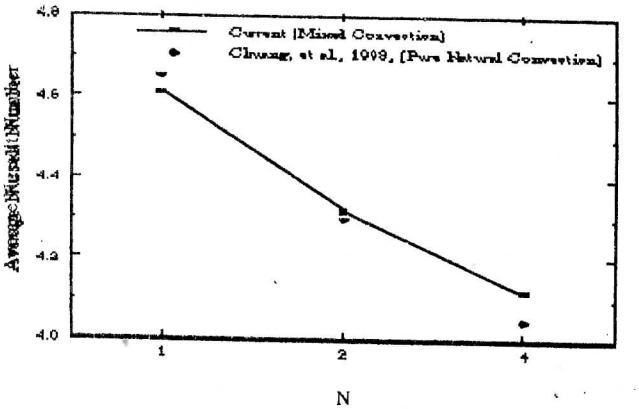

Figure 8 AVERAGE NUSSELT NUMBER vs N FOR AN ENCLOSURE WITH Ra = $3.55x10^5$.

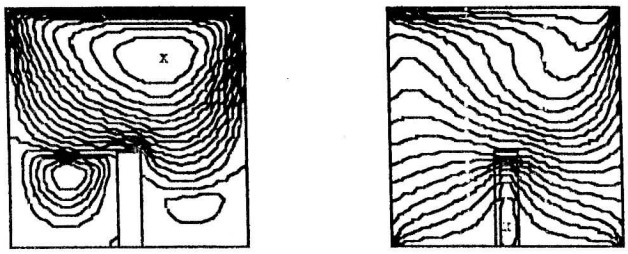

(a) (b)

Figure 9 STREAMLINES AND ISOTHERMS FOR TEST 2

Chuang, S., Chen, M., and Sun, C., 1993, "Numerical Study of Natural Convection in a Partitioned Enclosure," Proceedings of the 6th International Symposium on Transport Phenomena in Thermal Engineering, Seoul, Korea.

Duxbury, D.,1979, An Interferometric Study of Natural Convection in Enclosed Plane Air Layers with Complete and Partial Central Vertical Divisions, Ph.D. Thesis, University of Salford, U.K.

Gosman, A. D., Pum, W. N., Runchal, A. K., Spalding, D. B., and Wolfshtein M., 1969, Heat and Mass Transfer in Recirculating Flows, Academic Press, London.

Iwatsu, R., Hyun, J. M., and Kuwahara, K., 1992, "Convection in a Differentially-Heated Square Cavity with a Torsionally-Oscillating Lid," Int. J. Heat and Mass Transfer, Vol. 35, No. 5, pp. 1069-1076.

Lin, N. N., and Bejan, A., 1983, "Natural Convection in a Partially Divided Enclosure," Int. J. Heat Mass Transfer, Vol. 26, pp. 1867-1877.

Mohamad, A. A. and Viskanta, R., 199[illegible], "Transient Low Prandtl Number Fluid Convection in a Lid Driven Cavity, Numerical Heat Transfer," Part A, Vol. 19, pp. 187-205.

Morzynski, M. and Popiel, Cz. O., 1988, "Laminar Heat Transfer in a Two–Dimensional Cavity Covered by a Moving Wall," Numerical Heat Transfer, Vol. 13, pp 265-273.

Nansteel, M. W., and Grief,R., 1986, "An Investigation on Natural Convection in Enclosures with Two- and Three-Dimensinal Partitions," , Int. J. Heat Mass Transfer, Vol. 27, pp. 561-571.

Papanicolau, E. y Jaluria, Y., 1990, Conjugate Mixed Convection from Thermal Sources is a Rectangular Enclosure, in Simulations and Numerical Methods in Heat Transfer, A. F. Emery (ed.), ASME-HTD, Vol. 157, pp. 29-40.

Papanicolau, E. y Jaluria, Y., 1991, Convective Cooling of Multiple Electronic Components in an Enclosure, in Heat Transfer in Electronic Equipment, Ortega, A., Agonafer, D., y Webb, B. W. (eds), ASME-HTD, Vol. 171, pp. 29-37.

Patankar, S. V., 1980, Numerical Heat Transfer and Fluid Flow, McGraw-Hill, New York.

Ramesh, P. S. and Lean, M. H., 1992, "A Boundary Integral Formulation for Natural Convection Flows," Communications in Applied Numerical Methods, Vol. 8, pp. 407-415.

Sánchez, A., Krajewski, W. F., & Smith, T. F., 1992, A General Purpose Radiative Transfer Model for Application to Remote Sensing in Multi-Dimensional Systems, IIHR Report No. 355, Iowa Institute of Hydraulic Research, The University of Iowa, Iowa City, Iowa.

Sánchez, A. and Smith, T. F., 1992, Surface Radiation Exchange for Two-Dimensional Rectangular Enclosures Using the Discrete-Ordinates Method, J Heat Transfer, Vol. 114, No. 2, pp. 465-472

Sánchez, A., Morales, J. C., y Campo, A., 1993a, Application of the Discrete Ordinates Method to Buoyancy-Induced Radiating Fluids in a Square Enclosure with a Moving Wall, in General Papers in Radiative Heat Transfer, ASME-HTD, Vol. 257, pp. 25-32.

Sánchez A., A., Campo, A., and Morales C., J., 1993b, "Estudio Preliminar del Modelaje de los Efectos Combinados de Radiación/Convección en Cavidades con Frontera Movil y Protuberancias Internas con Generación de Calor," I Congreso de Ingeniería Mecánica, Mérida, Venezuela.

Sánchez A., A., Rosales R., Jiménez. de P., I., and Campo, A., 1994a, "Efectos Combinados de Radiación y Convección Mixta en el Enfriamiento de Componentes Electrónicos," Accepted for presentation at the XI Congreso Nacional de Ingeniería Mecánica, Valencia, España.

Sánchez A,. and A., Rosales R., 1994b, "Efectos Combinados de Radiación y Convección en el Enfriamiento de Componentes Electrónicos Generadores de Calor Colocados en Canales Bidimensionales," Accepted for presentation at the II Congreso Venezolano de Métodos Numéricos en Ingeniería y Ciencias Aplicadas, Maracaibo, Venezuela.

Torrance, K., Davis, R., Eike, K., Gill, P., Gutman, D., Hsui, A., Lyons, S., and Zien, H., 1972, "Cavity Flows Driven by Buoyancy and Shear," Journal of Fluid Mechanics, Vol. 51, pp. 221-231.

Yucel, A. and Acharya, S., 1990, "Natural Convection of a Radiating Fluid in a Partially Divided Square Enclosure," Eds. S. T. Thynell and J. R. Mahan, Radiation Heat Transfer, HTD-Vol. 154, A.S.M.E., pp. 19-28.

Zimmerman, E. and Acharya, S., 1987,"Free Convection Heat Transfer in a Partially Divided Vertical Enclosure with Conducting End Wall,",Int. J. Heat Mass Transfer, Vol. 30, pp. 319-331.